NOTES AND CORRESPONDENCE

Regional Patterns of Sea Level Change Related to Interannual Variability and Multidecadal Trends in the Atlantic Meridional Overturning Circulation*

K. LORBACHER, J. DENGG, C. W. BÖNING, AND A. BIASTOCH

IFM-GEOMAR, Leibniz-Institut für Meereswissenschaften, Kiel, Germany

(Manuscript received 10 July 2009, in final form 5 January 2010)

ABSTRACT

Some studies of ocean climate model experiments suggest that regional changes in dynamic sea level could provide a valuable indicator of trends in the strength of the Atlantic meridional overturning circulation (MOC). This paper describes the use of a sequence of global ocean–ice model experiments to show that the diagnosed patterns of sea surface height (SSH) anomalies associated with changes in the MOC in the North Atlantic (NA) depend critically on the time scales of interest. Model hindcast simulations for 1958–2004 reproduce the observed pattern of SSH variability with extrema occurring along the Gulf Stream (GS) and in the subpolar gyre (SPG), but they also show that the pattern is primarily related to the wind-driven variability of MOC and gyre circulation on interannual time scales; it is reflected also in the leading EOF of SSH variability over the NA Ocean, as described in previous studies. The pattern, however, is not useful as a "fingerprint" of longer-term changes in the MOC: as shown with a companion experiment, a multidecadal, gradual decline in the MOC [of 5 Sv (1 Sv $\equiv 10^6$ m^3 s^{-1}) over 5 decades] induces a much broader, basin-scale SSH rise over the mid-to-high-latitude NA, with amplitudes of 20 cm. The detectability of such a trend is low along the GS since low-frequency SSH changes are effectively masked here by strong variability on shorter time scales. More favorable signal-to-noise ratios are found in the SPG and the eastern NA, where a MOC trend of 0.1 Sv yr^{-1} would leave a significant imprint in SSH already after about 20 years.

1. Introduction

Global climate model simulations suggest the possibility of a gradual decline of the meridional overturning circulation (MOC) in the Atlantic Ocean during the twenty-first century (Meehl et al. 2007; Gregory et al. 2005). The projected reductions due to anthropogenic warming and freshening in the northern North Atlantic (NA) range from 0% to about 50%, not including the possible additional effects due to the enhanced melting of the Greenland ice sheet (Jungclaus et al. 2006). Since the strength of the MOC is intimately linked to the meridional transport of heat (Biastoch et al. 2008;

Rhines et al. 2008) and also affects the sequestration of carbon dioxide (Sarmiento and LeQuéré 1996; Biastoch et al. 2007) in the NA Ocean, a progressive weakening is expected to have major implications for the future evolution of climate (Bindoff et al. 2007), particularly for northwest Europe (Vellinga and Wood 2002).

The detection of a gradual change in the MOC is a challenging task for ocean-observing systems, involving the determination of trends in meridional velocity fields along transoceanic sections that are characterized by strong variability over a broad spectrum of space and time scales. Observational efforts have focused on the subtropical NA, particularly along 26.5°N where the presence of a well-defined western boundary current together with the structure of the interior temperature and salinity fields permits a determination of the MOC and the associated heat transport from individual hydrographic surveys to an accuracy of ±15%–20% (Bryden and Imawaki 2001). While historical occupations of this section—that is, the five repeats between 1957 and 2004 (Bryden et al. 2005)—are considered too

---

Corresponding author address: C. W. Böning, IFM-GEOMAR, Leibniz-Institut für Meereswissenschaften, Düsternbrooker Weg 20, 24105 Kiel, Germany.
E-mail: cboening@ifm-geomar.de

infrequent to avoid an aliasing of high-frequency variability in the calculation of long-term trends (Baehr et al. 2007; Wunsch 2008), the monitoring system established by the Rapid Climate Change–Meridional Overturning Circulation and Heatflux Array (RAPID–MOCHA) effort in March 2004 (Marotzke et al. 2009) has begun to provide a continuous record of the MOC transport at this latitude. However, the presence of vigorous variability on intraseasonal-to-interannual time scales (Cunningham et al. 2007; Kanzow et al. 2007) still poses a formidable challenge for the detection of long-term changes in the MOC, suggesting that continuous measurements over multidecadal time spans [>60 yr for an assumed observation error of 1 Sv (1 Sv $\equiv$ 10^6 m^3 s^{-1})] are required to detect a trend of the magnitude projected by the Intergovernmental Panel on Climate Change (IPCC) model results (Baehr et al. 2007).

Since the MOC is reflected in the near-surface current fields—for example, in the strength and position of the Gulf Stream (GS) and North Atlantic Current (NAC)—an important indirect indicator of MOC changes could be provided by regional patterns of sea surface height (SSH) anomalies associated with the dynamic adjustment of surface circulation features. Model studies noted that variability of the MOC is associated with pronounced regional changes in SSH, especially in the western NA (Bryan 1996; Häkkinen 2000), typically being characterized by a dipole (or, tripole) pattern of changes centered in the subpolar gyre (SPG) and along the GS/NAC, with weaker changes in the subtropical gyre (STG). A similar pattern was found in relation to interannual-to-decadal MOC variability in the leading empirical orthogonal function (EOF) of SSH anomalies simulated by a 1000-yr climate model control run by Zhang (2008), suggesting its potential use as a "fingerprint" of MOC strength. Modeling studies arrived at conflicting results, however, concerning the manifestation of long-term MOC trends in regional SSH patterns: while dynamic sea level change in an IPCC scenario run projecting a MOC decline of 25% was characterized by a similar dipole/tripole as stated earlier (Landerer et al. 2007), the simulation of a major MOC decline by Levermann et al. (2005) showed a very different pattern, with a much broader, basin-scale sea level rise over most of the NA.

In the study presented here, we use a sequence of ocean model experiments to demonstrate that to rationalize regional patterns of SSH anomalies and their association with MOC changes in the NA, it is of first importance to distinguish variability on interannual-to-decadal time scales from longer-term changes.

2. Model experiments

Our aim is to examine the manifestation in regional dynamic SSH patterns of a multidecadal decline in the MOC and to contrast these patterns with the natural SSH variability patterns on intraseasonal-to-decadal time scales due to atmospheric forcing and internal dynamic processes. Our modeling strategy is based on a sequence of global model experiments, involving a set of hindcast simulations (with and without eddies permitted) forced by atmospheric reanalysis products for 1958–2004, and a perturbation experiment in which the MOC is artificially forced to decline by imposing freshwater flux anomalies in the northern NA. The model experiments are based on different implementations of Nucleus for European Modelling of the Ocean (NEMO; Madec 2006), involving coupled ocean [Océan Parallélisé, version 9 (OPA9)]–sea ice [Louvain-la-Neuve Sea-Ice Model, version 2 (LIM2)] models in global-grid configurations [Oceanic Remote Chemical/Optical Analyzer (ORCA)] at ½° resolution (ORCA05; the grid spacing in the midlatitude NA is about 40 km) developed as part of the Drakkar collaboration (Barnier et al. 2007). The model uses 46 levels in the vertical; the bottom cells are allowed to be partially filled. The effect of explicitly simulated mesoscale eddies was assessed by a companion study with an eddy-permitting (¼°) configuration (ORCA025; Barnier et al. 2006). While showing a somewhat (~20%) stronger intraseasonal-to-interannual MOC variability than the control experiment (CNTRL), it indicated relatively minor effects of eddy dynamics on the concomitant, large-scale SSH patterns discussed in this paper. A presentation of results from the eddying model case is thus deferred to the supplementary material (Figs. S1–S4).

The surface boundary conditions use the formulations and datasets developed by Large and Yeager (2004) that have been taken as the basis for the "Coordinated Ocean–Ice Reference Experiments" (COREs) proposed by Griffies et al. (2009). The 6-hourly (wind, humidity, air temperature), daily (shortwave and longwave radiation), and monthly (freshwater fields) forcing data consist of a combination of National Centers for Environmental Prediction–National Center for Atmospheric Research (NCEP–NCAR) reanalysis products (Kalnay et al. 1996) with various satellite datasets and involve corrections for global imbalances. Turbulent fluxes are computed from bulk formulas as a function of the prescribed atmospheric state and the simulated ocean surface state. The spurious salinity drifts typically occurring under such conditions (cf. Griffies et al. 2009) are minimized by a relaxation of salinity to climatological conditions, adopting two different configurations: both versions use
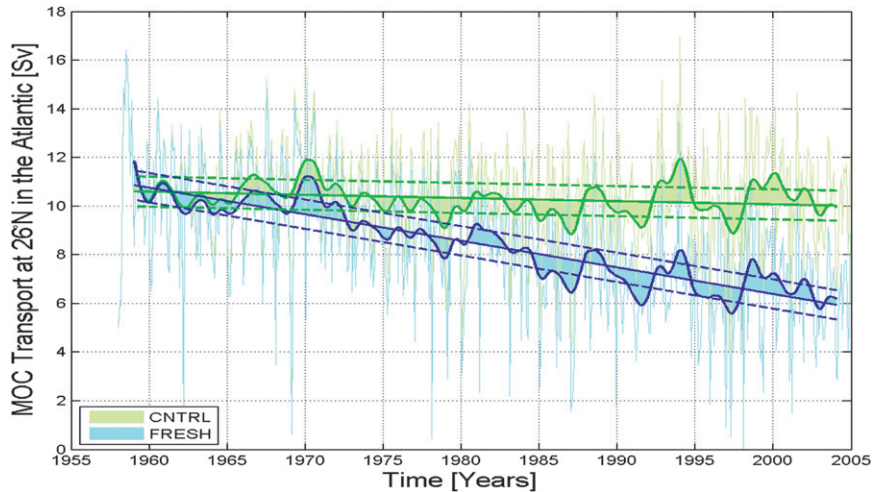
FIG. 1. Indices of large-scale transport variability. Maximum of the streamfunction of zonally integrated volume transport (MOC transport) at 26.5°N in CNTRL and FRESH: monthly-mean values (thin lines) and interannually smoothed with a 23-month Hanning filter (bold lines). Shading is relative to the long-term (1958–2004) linear trends (straight lines). Dashed lines mark plus or minus one standard deviation of annual mean anomalies. The simulations exhibit similar variability relative to the trends, with correlations of 0.98 for monthly values and 0.84 for smoothed values.

a "weak restoring" (with time scales of 180 and 360 days) of sea surface salinity (SSS) over the bulk of the domain; for the polar oceans, one version uses an enhanced restoring (time scale of 1 month) of SSS, the other version uses a "weak" (180 days) relaxation of salinity for the whole water column [as used before by Biastoch et al. (2008)]. Comparison of experiments with different restoring configurations showed little effects on the SSH variability patterns—that is, confirmed that the solution behaviors considered in this study are robust with respect to this aspect of the model configuration.

The main set of experiments consists of a hindcast simulation (CNTRL) of the atmopherically forced variability for 1958–2004 and a perturbation experiment (FRESH) in which a decline in the MOC is artificially induced by a 15%–20% increase of precipitation in the northern NA (corresponding to a zonal average of 0.15 m yr^{-1} or 0.08 Sv surplus in the freshwater flux). The imposed change in the freshwater budget leads to a declining trend in the MOC transport by about 5 Sv over the duration of the experiment (Fig. 1), without a substantial change in the vertical structure: Annual mean differences between CNTRL and FRESH of the streamfunction of meridional transport in years 1970 and 2000 show a weakening of the streamfunction, while its general structure, with its midlatitude maximum at about 1000-m depth, remains largely the same (not shown). The magnitude of the (artificially induced) trend is reminiscent of the MOC behavior in global

warming scenarios as discussed in Gregory et al. (2005). Note that despite the differences in the trends, the MOC variability is almost identical in the two runs, demonstrating the prime importance of the surface heat and momentum fluxes for the variability on interannual-to-decadal time scales as discussed by Biastoch et al. (2008). For a test of the robustness of the SSH signatures, and an assessment of their dynamical causes, we have included two additional experiments: 1) a sensitivity experiment (CNTRL-GM) in which eddy effects were parameterized following Gent and McWilliams (1990) and 2) a corresponding perturbation experiment with this configuration (WIND-GM) that is aimed at identifying the individual role of wind stress variability by using annually repeating seasonal climatologies for the heat and freshwater fluxes.

For the time tendency of dynamic changes of SSH, η, the model uses a prognostic (implicit time stepping) free surface formulation,

$$\frac{\partial \eta}{\partial t} = -\mathbf{V}_h \cdot \mathbf{U} - q_w,$$

$$\mathbf{U} = \int_{-H}^{\eta} \mathbf{u}_h \, dz, \quad \text{and} \quad \eta = \overline{\eta} + \eta_d,$$

where H is the ocean depth, $\mathbf{u}$ is the horizontal velocity, and q_w is the net surface freshwater flux. In our analysis we follow previous studies Levermann et al. 2005;
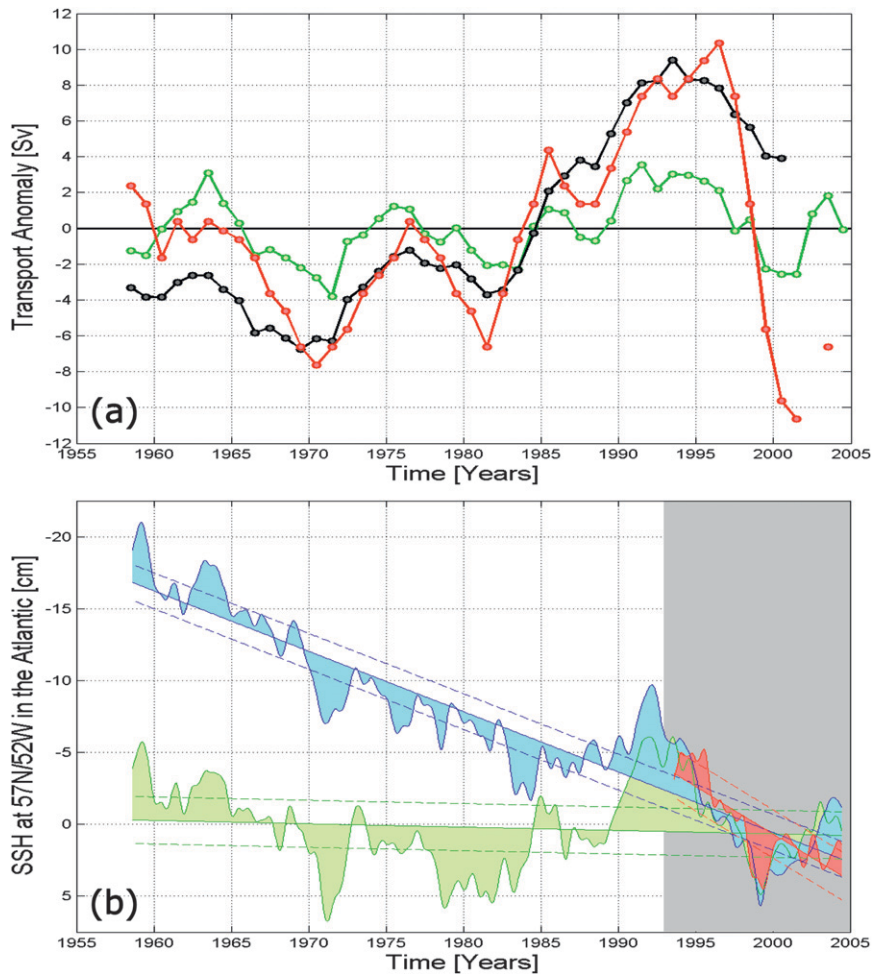
FIG. 2. Indices of large-scale transport variability. (a) Index of observed (red) annual mean baroclinic mass transport anomaly between the SPG and STG following Curry and McCartney (2001) in comparison to the model simulations CNTRL (green) and CNTRL-GM (black), whereby the amplitude of year-to-year variability amounts to 5.0 Sv in the observations, 1.8 Sv in CNTRL, and 3.8 Sv in CNTRL-GM. (b) SPG index following Häkkinen and Rhines (2004) and Hátún et al. (2005) as given by the annually smoothed monthly-mean sea level anomaly η_d at 57°N, 52°W in Archiving, Validation, and Interpretation of Satellite Oceanographic data (AVISO) satellite altimeter data (red), CNTRL (green), and FRESH (blue), with linear trends (solid) and standard deviations of interannual variability (dashed). Note that the climatological seasonal cycle over the period shaded in gray has been subtracted, resulting in a shift of these "normalized" time series to emphasize the similarity of interannual variability of both model cases and observational data.

Wunsch et al. 2007) and subtract a globally uniform, but time-varying value, $\overline{\eta}$, that reflects the net expansion/contraction of the global ocean (Greatbatch 1994) but has no dynamical effect. We refer to the adjusted sea level as *dynamic SSH*, η_d. As observational reference we use a gridded ($\frac{1}{3}°\times\frac{1}{3}°$ Mercator) product of 7-day averages of satellite altimeter SSH anomalies with respect to a several-year mean from which we also subtracted a global mean value (cf. Wunsch et al. 2007).

3. Assessment of midlatitude circulation variability

While the realism of the simulated MOC variability cannot be tested directly, observational records allow some assessment of the associated changes in the midlatitude circulation. A metric of prime importance for inspecting changes over the last 5 decades is provided by the index of baroclinic transport between Bermuda and the Labrador Sea proposed by Curry and McCartney (2001, hereafter CM-index), which reflects changes in
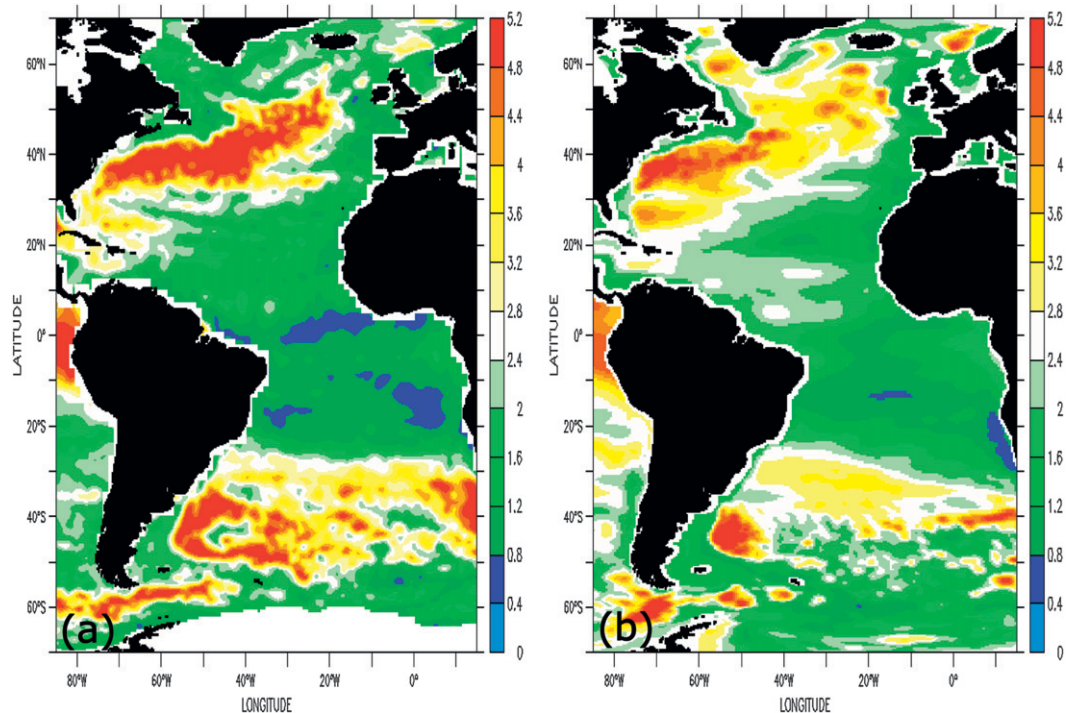
FIG. 3. Interannual sea level variability: model vs altimeter data. Standard deviation during 1993–2004 of annual mean anomalies of dynamic SSH, η_d (in cm): (a) AVISO data and (b) CNTRL.

the GS/NAC transport in the upper 2000 m (Fig. 2a). The hindcast simulations (CNTRL and CNTRL-GM) capture the observed rise of the CM-index from weak transports in the early 1970s to a maximum in the mid-1990s, and the subsequent decline to a minimum in 2001/02; correlations with the observed index are 0.77 for both CNTRL and CNTRL-GM. The main departure from the observed CM-index, and between the two hindcasts, lies in the amplitude of decadal variations (especially with regard to the transport maximum in the mid-1990s), which appears to be sensitive to model parameterization choices, that is, GM versus not GM [note that the companion, eddy-permitting model run shows a similar decadal behavior like CNTRL-GM after a spinup of 10 yr with similar amplitude (see Fig. S2)].

Changes in the intensity of the SPG are reflected in altimeter observations of SSH anomalies. A useful SPG-index (Häkkinen and Rhines 2004; Hátún et al. 2005) is provided by the principal component of an EOF analysis of η_d, or alternatively, by η_d, in the center of the Labrador Sea, where the cyclonic circulation is associated with a depression in mean sea level. A comparison of CNTRL with the observed time series of η_d in the central gyre is shown in Fig. 2b. A main signal in both is the rise by 8 cm between 1993 and 1999 that corresponds to a sharp decline in the SPG strength, with a partial

recovery thereafter (Böning et al. 2006). We note that over such a short period, the simulated η_d in FRESH is not significantly different: it is only for time spans longer than ~15 yr that the trend in FRESH becomes manifest; over 5 decades the MOC decline in that case leads to a rise in η_d of about 20 cm.

4. Spatial pattern of interannual-to-decadal SSH variability

Having established the model's fidelity in simulating observational indices of midlatitude circulation variablity, we now examine the spatial η_d variability patterns. We begin by assessing the simulated signatures with satellite altimeter data since 1993, before proceeding to the question of the manifestation of MOC changes on different time scales. The standard deviation of η_d over the period 1993–2004 in CNTRL is characterized by a similar distribution as in the observations (Fig. 3): highest amplitudes are associated with major frontal regions such as the GS/NAC (and the Malvinas Current/Zapiola anticyclone in the South Atlantic), suggesting that the interannual variability of η_d is concentrated in the same regions as the high-frequency variability, and thus reminiscent of the distribution of eddy variability in the Atlantic Ocean (e.g., Fu and Smith 1996).
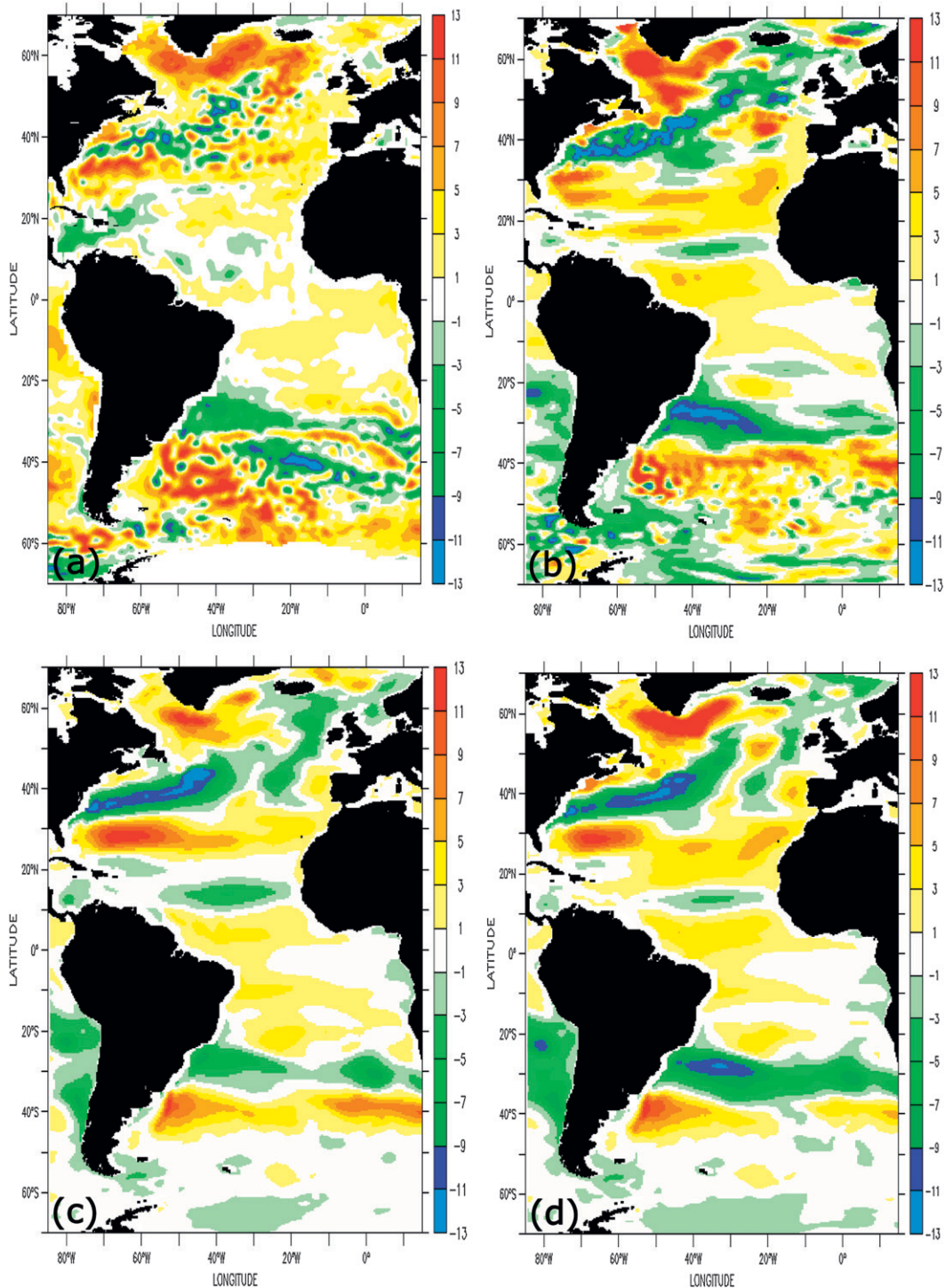
FIG. 4. Interannual sea level trend: model vs altimeter data. Linear trend (1993–1999) of η_d (in mm yr^{-1}) in comparison between (a) AVISO data and simulations, (b) CNTRL, (c) WIND-GM, and (d) CNTRL-GM.

The spatial distribution in the midlatitude NA of the changes in η_d during the 1990s has been analyzed in several studies, and is described as a basinwide coherent dipole structure between the subpolar and subtropical NA; it changed sign between 1995 and 1996 in response to a sharp drop in the North Atlantic Oscillation (NAO) index (Esselborn and Eden 2001, hereafter EE01). The dipole (or rather, tripole) pattern is clearly exhibited by
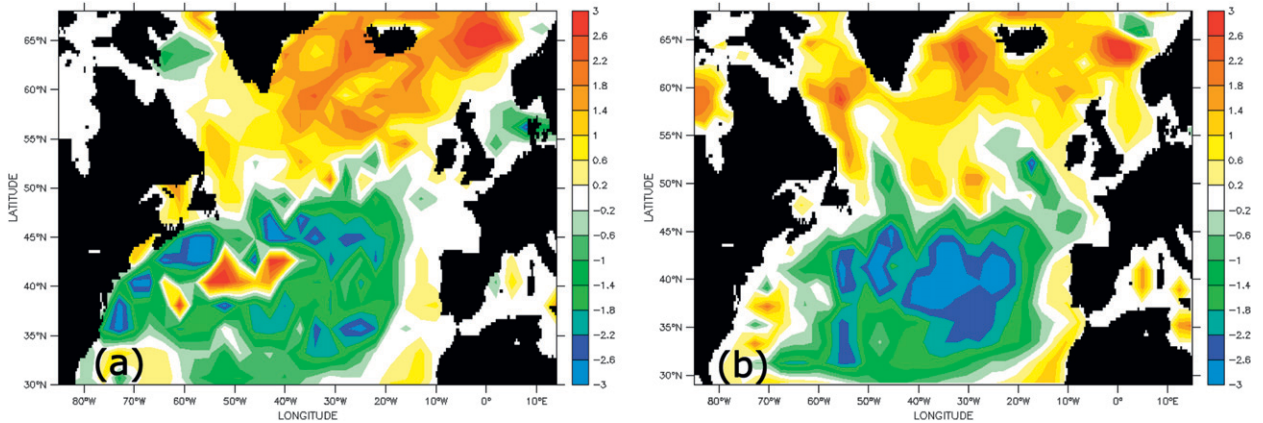
FIG. 5. Patterns of interannual sea level variability. First EOF of detrended anomalous annual means of η_d over the observational period (1993–2004) in (a) AVISO data and (b) CNTRL.

the linear trend of η_d in the midlatitude NA during 1993–99 (Fig. 4a), the period of the strong decline in the SPG-index (Fig. 2b): η_d changes are positive in the SPG, while negative values dominate along the path of the GS/NAC and, in turn, weak positive values in the STG. The main observed features are already well reproduced in the hindcast simulations at ½° resolution (Fig. 4); the eddy-permitting (¼°) simulation exhibits an increased fidelity in reproducing smaller-scale features, such as

the SSH variations in the northwest corner as well as along the GS/NAC path (refer to supplemental material). In contrast, the adoption of GM mixing (Figs. 4b,d), which effectively suppresses the generation of mesoscale eddies in the ¼° case, leads to smoother patterns than in CNTRL (Fig. 4c). From the comparable set of simulations, we can conclude that the model captures the salient aspects of the decadal circulation variability in the midlatitude NA.
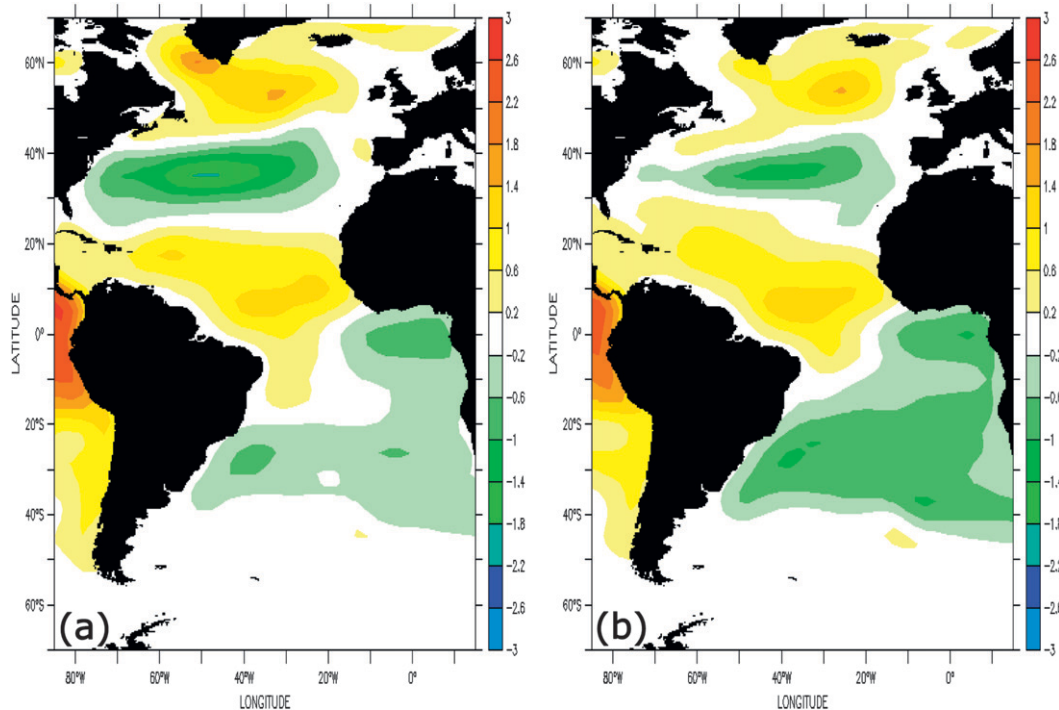

FIG. 6. Dynamic cause of interannual sea level variability patterns. First EOF of detrended anomalous annual means of η_d over the hindcasting period (1958–2004) in (a) CNTRL-GM and (b) WIND-GM.

This level of skill is also exhibited by an EOF analysis of (detrended) η_d time series, where the leading mode for 1993–2004 in CNTRL is almost indistinguishable from the observational pattern for this period (Fig. 5), explaining 31% of the variance in both cases. Note that the EOF patterns and amplitudes of FRESH of the original η_d time series during the 1990s are very similar to CNTRL, although the MOC in that case has weakened by 50%: it gives a first indication that this pattern is related to interannual circulation changes and not much influenced by longer-term trends. Over the extended period of the model simulation—that is, from 1958 to 2004—the first EOF (Fig. 6) explains 22% of the variance and exhibits a large-scale pattern of alternating changes in the SPG (north of ~40°N), midlatitudes (~25°–40°N), and tropical NA that matches the results discussed in previous studies (e.g., Häkkinen 2001, Häkkinen and Rhines 2004; Zhang 2008).

A question of interest in the present study is whether this η_d pattern can be attributed to buoyancy-driven, large-scale MOC changes in the North Atlantic or whether it is due to other dynamical causes. EE01 has attributed the dynamic nature of the SSH variability signal during the 1990s to a redistribution of upper-ocean heat content associated with a fast dynamical response of the circulation to a drop in the NAO index in the mid-1990s. Idealized model experiments (EE01; Eden and Willebrand 2001) suggested a primary role of the wind stress in inducing SSH anomalies on time scales of a few years. These findings are confirmed and extended by experiment WIND-GM: the purely wind-driven changes in η_d during 1993–99 (Fig. 4c) suffice to reproduce the large-scale pattern of the reference solution over the whole Atlantic Ocean (Fig. 4b); the same is true for the leading EOF of the wind-driven variability over the whole simulation period, 1958–2004 (Fig. 6).

5. SSH pattern related to a multidecadal MOC decline

In contrast to the alternating η_d pattern related to interannual-to-decadal variability of the wind stress, a distinctly different distribution emerges as a result of the multidecadal MOC decline simulated in FRESH: the η_d trend in that case (Fig. 7) shows a rise in sea level over the whole NA, with a broad maximum of about 5 mm yr^{-1} spanning the SPG and parts of the NAC, contrasted by somewhat weaker decreases of 2 mm yr^{-1} in the Southern Hemisphere. The dominant feature of the η_d change after 5 decades of MOC decline is thus a positive south–north gradient of about 20 cm in the Atlantic Ocean, reflecting a pronounced interhemispheric
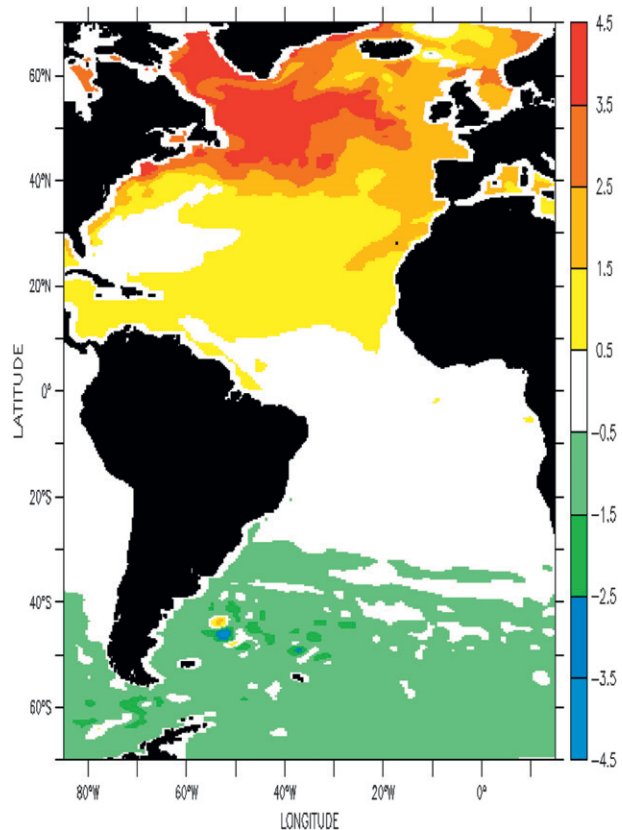

FIG. 7. SSH changes due to multidecadal MOC decline. Linear trend (1958–2004) of η_d (in mm yr^{-1}) in FRESH relative to CNTRL.

mass redistribution, as in the climate modeling results of Levermann et al. (2005). An interesting regional-scale feature that was also noted in recent studies of IPCC scenario runs by Yin et al. (2009) and Hu et al. (2009) is the wedge of rising sea levels that extends southward from the SPG along the American coast to about 35°N.

The simulated η_d trend pattern in FRESH (Fig. 7) is very similar to the leading EOF pattern of the un-filtered (no temporal linear trend removed) annual mean η_d variability. By explaining 67% of the variance in the NA, it is clearly the dominant pattern of multidecadal variability of η_d in this experiment. A statistical com-parison of the unfiltered multivariate η_d variability between WIND-GM and FRESH, following the meth-odology of Dommenget (2007), confirms that the pattern related to the MOC trend differs significantly from the pattern of wind-driven variability. The structure of the MOC-related η_d trend in FRESH reflects a weakening of the eastward currents in the northern/southern mid-latitudes. The weakening of the NAC is consistent with the declining CM-index seen in Fig. 2a; it also indicates
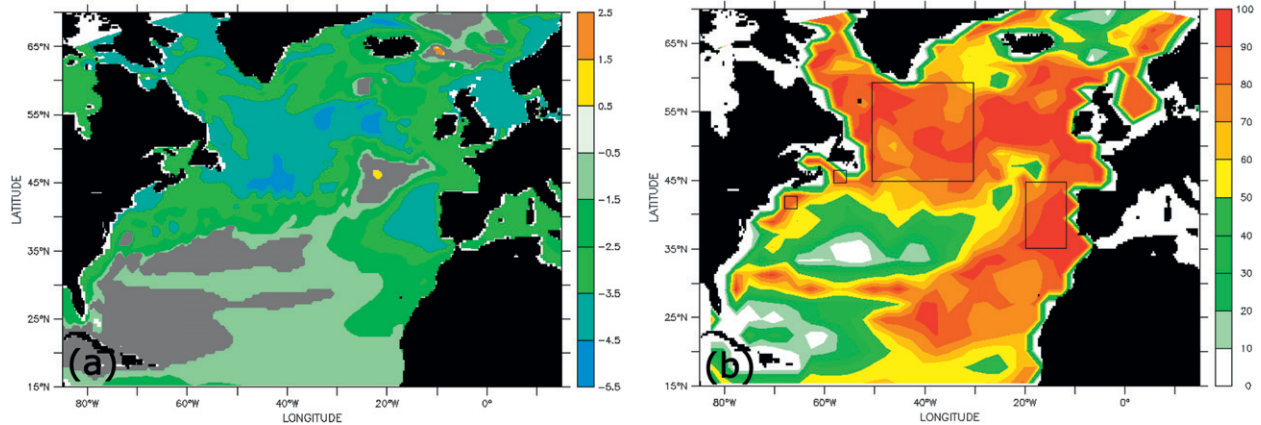
FIG. 8. Manifestation of multidecadal MOC decline. (a) Linear regression (1958–2004) of anomalous annual mean η_d and the MOC index in FRESH (in cm Sv^{-1}); gray areas indicate nonsignificant values at the Student's t test 95% level. (b) Percentage of the covariance between local η_d and the MOC index due to the linear trends in both variables. Boxes indicate regions where we have assessed the detectability of a gradual MOC decline as simulated in FRESH based on continuous records of η_d (Labrador Sea: 57°N, 52°W; SPG: average from 45°–60°N to 30°–50°W, "west European" box: average from 35°–45°N to 12°–22°W, and two sites along the North American coast: 41°–43°N, 65°–68°W and 45°–46°N, 56°–58°W).

an overall weakening of the SPG, and a weaker STG circulation in the eastern NA (i.e., weaker Canary Current and North Equatorial Current).

Having established the η_d signatures of a multidecadal MOC decline, we now turn to address the issue of its detectability in the real ocean. More specifically, can the signature of a gradual MOC-related trend be detected against the presence of higher-frequency "noise" associated with wind-driven and internal dynamic processes? We first assess the manifestation of MOC variability in regional SSH changes by examining the linear regression of η_d onto the MOC transport at 26°N in FRESH (Fig. 8a). Maximum regression values of -4.5 cm Sv^{-1} (significant at the 95% level) are found in the SPG and also along the west European coast. The

distribution is reminiscent of previous findings obtained from a different (coarse-resolution climate) model and approach by Levermann et al. (2005).

To determine if these regression patterns are primarily caused by the interannual variability or the trend of the MOC, we computed the percentage of the trend-induced contribution to the covariance. The relative contribution of a linear trend (signal) and internal variability (noise) to the SSH–MOC regression is obtained by utilizing symmetry properties for the covariance of two variables (von Storch and Zwiers 1999): by decomposing the complete covariance into the sum of the covariances of the linear trends and of the deviations (residuals) from the trends, a percentage expression for the trend-induced covariance

$$r_{\text{trend}} = \frac{\left\|\text{cov}[\text{trend}(x_1), \text{trend}(x_2)]\right\|}{\left\|\text{cov}(x_1' x_2')\right\| + \left\|\text{cov}[\text{trend}(x_1), \text{trend}(x_2)]\right\|} \times 100$$

is obtained, where x_1 and x_2 stand for the two time series and the prime for the pointwise temporal-trend-removed time series.

On the basis of this analysis, we can identify the regions where the relative effect of the long-term MOC change dominates the η_d variability in FRESH (Fig. 8b): particularly high values are found for a "horseshoe" pattern with maxima of >80% from the SPG along the west European coast. The long-term MOC trend manifests itself also (with values of more than 50%) along the inshore side of the GS, consistent with recent results of

Hu et al. (2009). In contrast, the trend contribution is less than 50% along the offshore side of the GS, implying that this region is not a sensitive indicator for long-term MOC changes.

Having determined where a significant MOC imprint can be expected, the question remains: After what observation period could such a trend be detected against the background of high-frequency (intraseasonal to interannual) SSH variability? To assess the significance of a trend signal, we use the Student's t test (e.g., von Storch and Zwiers 1999):

$$r_{x_1,t} = \pm \frac{T(N)}{\sqrt{T^2(N) + N(t)}},$$

which determines the correlation r between a time series x_1 and the time t in terms of the ratio of T (critical value from the t distribution) and the number of the degrees of freedom N (the number of independent samples). We estimate N by the time lag at which the autocorrelation function of η_d in CNTRL drops below 0.2: it gives periods of 3.5 yr for the Labrador Sea, 4.5 yr for the SPG, 7 yr for a "west European" box, and 2.5 yr for two boxes along the North American coast (for the definition of the boxes, see Fig. 8b). From this we obtain minimum periods for a significant detection (at the 95% level) of the trend signal in FRESH of 16 yr for the SPG and 24 yr for the west European box; in contrast, a significant trend detection based on the SSH changes along the North American coast would require periods longer than the model integration time of 47 yr. It is interesting to note that the detection times are not significantly affected by the box sizes—for example, there is only little difference between the estimates for the SPG box and the single station point in the center of the Labrador Sea. An application to the real ocean would, in addition, need to account for SSH measurement errors; more specifically, the detection periods would increase to 19 yr (SPG) and 31 yr (west European box) by assuming an altimeter measurement uncertainty of 2 cm.

6. Concluding discussion

The model study suggests repercussions of a gradual decline (of 5 Sv over 5 decades in this study) in MOC strength on SSH anomaly fields that are in marked contrast to the dipole pattern of interannual SSH anomalies described in previous studies. Our analysis shows that the latter signature, with the strongest SSH anomalies along the GS and NAC, can be attributed mainly to the response of ocean circulation to changes in wind stress. In contrast, the dynamical effect on SSH of a longer-term trend in the MOC associated with a decline in subarctic deep-water formation is a broad SSH rise in the NA and a broad SSH fall in the Southern Hemisphere. A similar interhemispheric seesaw has been reported in coarse-resolution climate model runs and rationalized in terms of a large-scale redistribution of mass, that is, an adiabatic adjustment in the ocean's density structure (Levermann et al. 2005).

The difference in SSH patterns suggests that over the midlatitude NA, the manifestation of changes in MOC transport critically depends on the time scales of interest. A general implication is that trend studies of SSH

patterns based on available, relatively short (13 yr) altimeter records (Bindoff et al. 2007; Cromwell et al. 2007; Polito and Sato 2008) have to be interpreted with caution, especially along the GS in the midlatitude western North Atlantic, where the SSH variability is dominated by strong intraseasonal-to-interannual fluctuations. Because of this intense, high-frequency noise in SSH time series, the manifestation of a gradual trend in the MOC would effectively be masked in the GS regime. In this regard our ocean model analysis challenges previous conclusions drawn from coarse-resolution climate model simulations that suggested a significant imprint of a possible future MOC decline on sea level trends along the North American coast (Hu et al. 2009).

A much more favorable signal-to-noise ratio of a long-term MOC trend is found in the SPG and eastern NA, suggesting that an index of SSH changes in these regions could potentially provide a valuable contribution to an effective MOC monitoring system. More specifically, our model results suggest that a 0.1 Sv yr^{-1} decline in the MOC strength (a rate similar to projections from IPCC climate scenario simulations for the twenty-first century) corresponds to an SSH anomaly signal that would stand out against the high-frequency, primarily wind-driven, and internally generated (eddy) noise after about 20–30 yr in the SPG and eastern NA. This time scale also implies that if changes in the MOC were underway already as suspected in some studies (Bryden et al. 2005), it should only be a few years before the record of altimeter observations of SSH would cross the threshold for detectability of such a trend.

REFERENCES

Baehr, J., K. Keller, and J. Marotzke, 2007: Detecting potential changes in the meridional overturning circulation at 26°N in

the Atlantic. *Climate Change,* **91,** 11–27, doi:10.1007/s10584-006-9153-z.

Barnier, B., and Coauthors, 2006: Impact of partial steps and momentum advection schemes in a global ocean circulation model at eddy-permitting resolution. *Ocean Dyn.,* **56,** 543–567, doi:10.1007/s10236-006-0082-1.

——, and Coauthors, 2007: Eddy-permitting ocean circulation hindcasts of past decades. *CLIVAR Exchanges,* No. 42, International CLIVAR Project Office, Southampton, United Kingdom, 8–10.

Biastoch, A., C. Völker, and C. W. Böning, 2007: Uptake and spreading of anthropogenic trace gases in an eddy-permitting model of the Atlantic Ocean. *J. Geophys. Res.,* **112,** C09017, doi:10.1029/2006JC003966.

——, C. W. Böning, J. Getzlaff, J.-M. Molines, and G. Madec, 2008: Causes of interannual–decadal variability in the meridional overturning circulation of the midlatitude North Atlantic Ocean. *J. Climate,* **21,** 6599–6615.

Bindoff, N. L., and Coauthors, 2007: Observations: Oceanic climate change and sea level. *Climate Change 2007: The Physical Science Basis,* S. Solomon et al., Eds., Cambridge University Press, 385–432.

Böning, C. W., M. Scheinert, J. Dengg, A. Biastoch, and A. Funk, 2006: Decadal variability of subpolar gyre transport and its reverberation in the North Atlantic overturning. *Geophys. Res. Lett.,* **33,** L21S01, doi:10.1029/2006GL026906.

Bryan, K., 1996: The steric component of sea level rise associated with enhanced greenhouse warming: A model study. *Climate Dyn.,* **12,** 545–555.

Bryden, H. L., and S. Imawaki, 2001: Ocean heat transport. *Ocean Circulation and Climate: Observing and Modelling the Global Ocean,* G. Siedler et al., Eds., Academic Press, 455–474.

——, H. R. Longworth, and S. A. Cunningham, 2005: Slowing of the Atlantic meridional overturning circulation at 25°N. *Nature,* **438,** 655–657, doi:10.1038/nature04385.

Cromwell, D., A. G. P. Shaw, P. Challenor, R. E. Houseago-Stokes, and R. Tokmakian, 2007: Towards measuring the meridional overturning circulation from space. *Ocean Sci.,* **3,** 223–228.

Cunningham, S. A., and Coauthors, 2007: Temporal Variability of the Atlantic Meridional Overturning Circulation at 26.5°N. *Science,* **317,** 935–938, doi:10.1126/science.1141304.

Curry, R. G., and M. S. McCartney, 2001: Ocean gyre circulation changes associated with the North Atlantic Oscillation. *J. Phys. Oceanogr.,* **31,** 3374–3400.

Dommenget, D., 2007: Evaluating EOF modes against a stochastic null hypothesis. *Climate Dyn.,* **28,** 517–531, doi:10.1007/s00382-006-0195-8.

Eden, C., and J. Willebrand, 2001: Mechanism of interannual to decadal variability of the North Atlantic circulation. *J. Climate,* **14,** 2266–2280.

Esselborn, S., and C. Eden, 2001: Sea surface height changes in the North Atlantic Ocean related to the North Atlantic Oscillation. *Geophys. Res. Lett.,* **28,** 3473–3476.

Fu, L., and R. Smith, 1996: Global ocean circulation from satellite altimetry and high-resolution computer simulation. *Bull. Amer. Meteor. Soc.,* **77,** 2625–2636.

Gent, P. R., and J. C. McWilliams, 1990: Isopycnal mixing in ocean circulation models. *J. Phys. Oceanogr.,* **20,** 150–155.

Greatbatch, R., 1994: A note on the representation of steric sea level in models that conserve volume rather than mass. *J. Geophys. Res.,* **99** (C6), 12 767–12 771.

Gregory, J. M., and Coauthors, 2005: A model intercomparison of changes in the Atlantic thermohaline circulation in response to increasing atmospheric CO_2 concentration. *Geophys. Res. Lett.,* **32,** L12703, doi:10.1029/2005GL023209.

Griffies, S., and Coauthors, 2009: Coordinated Ocean-ice Reference Experiments (COREs). *Ocean Modell.,* **26,** 1–46, doi:10.1016/j.ocemod.2008.08.007.

Häkkinen, S., 2000: Decadal air–sea interaction in the North Atlantic based on observations and modeling results. *J. Climate,* **13,** 1195–1219.

——, 2001: Variability in the sea surface height: A qualitative measure for the meridional overturning in the North Atlantic. *J. Geophys. Res.,* **106** (C7), 13 837–13 848.

——, and P. B. Rhines, 2004: Decline of Subpolar North Atlantic Circulation During the 1990s. *Science,* **304,** 555–559, doi:10.1126/science.1094917.

Hátún, H., A. B. Sandø, H. Drange, B. Hansen, and H. Valdimarsson, 2005: Influence of the Atlantic Subpolar Gyre on the Thermohaline Circulation. *Science,* **309,** 1841–1844.

Hu, A., G. A. Meehl, W. Han, and J. Yin, 2009: Transient response of the MOC and climate to potential melting of the Greenland Ice Sheet in the 21st century. *Geophys. Res. Lett.,* **36,** L10707, doi:10.1029/2009GL037998.

Jungclaus, J. H., H. Haak, M. Esch, E. Roeckner, and J. Marotzke, 2006: Will Greenland melting halt the thermohaline circulation? *Geophys. Res. Lett.,* **33,** L17708, doi:10.1029/2006GL026815.

Kalnay, E., and Coauthors, 1996: The NCEP/NCAR 40-Year Reanalysis Project. *Bull. Amer. Meteor. Soc.,* **77,** 437–471.

Kanzow, T., and Coauthors, 2007: Observed Flow Compensation Associated with the MOC at 26.5°N in the Atlantic. *Science,* **317,** 938–941, doi:10.1126/science.1141293.

Landerer, F. W., J. H. Jungclaus, and J. Marotzke, 2007: Regional dynamic and steric sea level change in response to the IPCC-A1B scenario. *J. Phys. Oceanogr.,* **37,** 296–312.

Large, W. G., and S. G. Yeager, 2004: Diurnal to decadal global forcing for ocean and sea-ice models: The data sets and flux climatologies. NCAR Tech. Note NCAR/TN-460+STR, 112 pp.

Levermann, A., A. Griesel, M. Hoffmann, M. Montoya, and S. Rahmstorf, 2005: Dynamic sea level changes following changes in the thermohaline circulation. *Climate Dyn.,* **24,** 347–354, doi:10.1007/s00382-004-0505-y.

Madec, G., 2006: NEMO: The OPA ocean engine. IPSL Note du Pole de Modelisation, 110 pp.

Marotzke, J., S. A. Cunningham, and H. L. Bryden, cited 2009: Monitoring the Atlantic meridional overturning circulation at 26.5°N. [Available online at http://www.noc.soton.ac.uk/rapidmoc/home.html.]

Meehl, G. A., and Coauthors, 2007: Global climate projections. *Climate Change 2007: The Physical Science Basis,* S. Solomon et al., Eds., Cambridge University Press, 747–845.

Polito, P. S., and O. T. Sato, 2008: Global interannual trends and amplitude modulations of the sea surface height anomaly from the TOPEX/*Jason-1* altimeters. *J. Climate,* **21,** 2824–2834.

Rhines, P., S. Häkkinen, and S. A. Josey, 2008: Is oceanic heat transport significant in the climate system? *Arctic-Subarctic Ocean Fluxes: Defining the Role of the Northern Seas in Climate,* R. R. Dickson, J. Meincke, and P. Rhines, Eds., Springer, 87–109.

Sarmiento, J. L., and C. LeQuéré, 1996: Oceanic carbon dioxide uptake in a model of century-scale global warming. *Science,* **27,** 1346–1350.

Vellinga, M., and R. A. Wood, 2002: Global climate impacts of a collapse of the Atlantic thermohaline circulation. *Climatic Change,* **54,** 251–267.

von Storch, H., and F. W. Zwiers, 1999: *Statistical Analysis in Climate Research,* Cambridge University Press, 484 pp.

Wunsch, C., 2008: Mass and volume transport variability in an eddy-filled ocean. *Nat. Geosci.,* **1,** 165–168, doi:10.1038/ngeo126.

——, R. M. Ponte, and P. Heimbach, 2007: Decadal trends in sea level patterns: 1993–2004. *J. Climate,* **27,** 5889–5911.

Yin, J., M. E. Schlesinger, and R. J. Stouffer, 2009: Model projections of rapid sea-level rise on the northeast coast of the United States. *Nat. Geosci.,* **2,** 262–266, doi:10.1038/NGEO462.

Zhang, R., 2008: Coherent surface-subsurface fingerprint of the Atlantic meridional overturning circulation. *Geophys. Res. Lett.,* **35,** L20705, doi:10.1029/2008GL035463.